Engineered Science
DOI: https://dx.doi.org/10.30919/es1562

Geospatial Visualization of Logarithmic Attenuation of Pile-Driving Noise Based on Field Measurements

Yelbek Utepov,[1,*] Assel Mukhamejanova,[1,*] Aida Nazarova,[2] Aleksej Aniskin,[3] Aigul Kozhas[4] and Alisher Imanov[1,*]

Abstract

Pile-driving operations in construction generate intense pulsed noise, creating safety problems at the construction site and potentially causing concern in nearby communities. This study presents field measurements of sound pressure levels (SPL) from active pile driving at various distances, modeling decay using a logarithmic attenuation function and integrating the results with geospatial visualization. The measured time history of the SPL showed periodic fluctuations (amplitude ~17 dB) corresponding to the hammer impact cycle. By applying a logarithmic model (with distances calculated using the Haversin equation) to each measurement interval, we obtained attenuation coefficients that provided a high degree of confidence (R^2 > 0.8 in 77.5% of cases; the maximum value is 0.97). The model's predictions corresponded to the observed SPL values with an average error of about 2.6% and minor deviations (underestimation over medium distances). A noise map was compiled throughout the site, and 3D visualization was performed, identifying areas exceeding 85 dB near the source that require hearing protection and showing a decrease in SPL to safe levels (~55 dB) at the site boundary. These results demonstrate a novel integration of empirical measurements with logarithmic modeling and geospatial mapping to support construction noise assessment and protective zone planning.

Keywords: Pile-driving noise; Sound pressure level; Noise propagation; Logarithmic attenuation.
Received: 27 March 2025; Revised: 20 April 2025; Accepted: 20 May 2025.
Article type: Research article.

1. Introduction

Noise pollution is of increasing concern worldwide and has well-documented effects on public health, including irritation, sleep disorders, cardiovascular stress, cognitive impairment, and hearing loss.[1–4] Urban areas are particularly affected, where traffic, industrial, and construction work create high levels of noise that accumulate over time.[2,4,5] In both developing and developed cities, construction noise has become a significant factor in noise pollution in society, which has led to complaints, regulatory restrictions, and research to reduce it.[5–7] Recent global health assessments have highlighted the urgent need to combat urban noise – for example, constant exposure to noise above 70 dB is associated with hypertension and other adverse effects,[2,3] and construction sites are often hotbeds of such high-level noise. Sound pressure levels (SPL) that are significantly higher than the threshold safe for humans regularly occur at construction sites. Field measurements at operating construction sites have shown equivalent noise levels in the range of 80-100 dB or more near operating equipment.[6,7] In one study, peak levels of construction noise increased from 72 dB at the edge of the construction site to over 90 dB during heavy machinery operation.[6] Similarly, measurements at the sites of high-rise buildings have shown that typical noise from equipment can reach 95-100 dB over short distances.[7] Such levels are comparable to those observed in other noisy industrial activities – even short-term but intense noise from infrastructure construction (for example, drilling and blasting for oil/gas wells) has been shown to increase environmental noise levels in surrounding communities to potentially dangerous levels.[8] Among the sources of construction noise, the impact driving of piles stands out, especially for its impulsive nature and intensity. Pile driving involves repetitive high-amplitude pulses when the hammer hits the pile, creating

[1] *Department of Civil Engineering, L.N. Gumilyov Eurasian National University, Astana, 010008, Kazakhstan*
[2] *Department of Physics, Nazarbayev University, Astana, 010000, Kazakhstan*
[3] *Department of Civil Engineering, University North, Varazdin, 42000, Croatia*
[4] *Department of Technology of Industrial and Civil Engineering, L.N. Gumilyov Eurasian National University, Astana, 010008, Kazakhstan*
**Email:* utepov-elbek@mail.ru (Y. Utepov); assel.84@list.ru (A. Mukhamejanova); glad.alisher@gmail.com (A. Imanov)

sharp noise peaks that can exceed 110-120 dB at close range.[9] A field study of the noise from driven piles at the construction site showed that the noise level may keep at 100 dB level at a close distance of 20 m.[10] These pulsed noise bursts also create characteristic periodic fluctuations in the time histories of the measured SPL, as observed in experimental studies.[11] For example, it has been shown that pulsed noise from pile driving causes rapid fluctuations in SPL by 15-25 dB with a frequency corresponding to the frequency of hammer blows.[12] Such characteristics are markedly different from stable continuous noise and can increase the subjective irritating and frightening potential for both construction workers and residents of close neighborhoods. Indeed, recent studies of the sound environment in construction show that impulsive, intermittent noises are usually rated as more disturbing than constant noise of the same average level.[13,14]

In addition to disturbing public order, construction noise poses a serious danger to workers. Long-lasting occupational exposure to high noise levels in construction is associated with increased levels of hearing loss and noise-related injuries. Epidemiological studies have shown that the prevalence of hearing impairments among construction workers is significantly higher compared to most other industries in similar age groups.[15] A longitudinal analysis of US workers has shown that the construction sector has consistently occupied one of the first places in terms of the incidence of hearing loss in the workplace for three decades.[15] Excessive noise can also mask danger or communication, contributing to accidents; a meta-analysis has shown that high noise levels in the workplace double the risk of occupational injury due to mechanisms such as reduced awareness and fatigue.[14] Despite the availability of personal hearing protection and safety regulations, their effectiveness on construction sites is often limited. Surveys show that many construction workers do not wear hearing protection equipment all the time or incorrectly, which leads to only a partial reduction in noise exposure.[16,17] Even with protective measures, pulse noises can still be transmitted as harmful peaks; standard dose measurements may underestimate the impact of transient sound pressure surges.[14] Field studies in Asia also show that a significant proportion of construction work produces noise above 85 dB despite efforts to reduce exposure. For example, a study in Beijing showed that most heavy equipment operations and even some finishing work regularly exceed the safe exposure limits set by the authorities.[18] These data indicate that without additional control measures, construction crews are still at risk of harm to health due to noise.

Given the importance of construction noise, numerous studies have attempted to characterize its distribution and develop predictive models for noise levels at various distances.[19-21] In general, sound from an external point source decays with distance in accordance with the geometric law of propagation (approximately 6 dB per doubling of the distance in a free field).[16,17] Real-world measurements often follow this logarithmic attenuation trend, although with deviations due to reflections, absorption by the earth, and other factors. The researchers used empirical approaches to construct attenuation curves at a distance for building noise data, obtaining models for a specific object in the form $L(d)=L_0-a*\log10(d)$ (where "a" is about 20 with ideal propagation).[22] Simple logarithmic regression models have been successfully applied to building noise datasets to estimate how quickly levels decrease with increasing range.[22] In addition to basic regression models, more sophisticated forecasting methods have been explored. For example, artificial neural network models have been trained based on construction noise measurements to predict noise levels based on factors such as equipment type, distance, and barriers.[23] Such data-based models can reflect complex interactions (for example, multiple simultaneous sources or partial shielding) better than purely theoretical formulas.[24] On the other hand, physics-based modeling tools are also widely used to predict environmental noise. Standardized algorithms (such as in ISO 9613-2) are implemented in noise mapping software to account for distance attenuation,[25] atmospheric absorption, earth influence, and obstacle diffraction.[26,27] These tools, originally developed for transport and industrial noise, have been applied to construction scenarios to predict the noise impact in the far zone.[28] For example, Reed *et al*.[26] have developed a noise propagation tool integrated into GIS that can take into account soil and vegetation cover and topography, which increases the accuracy of predicting outdoor noise levels. Similarly, open-source platforms now allow for the inclusion of advanced propagation models (including reflections and frequency-dependent attenuation) directly into geographic information systems to create noise maps.[29,30]

A key achievement in recent years has been the integration of geographic data and sensor networks to monitor construction noise in real time. GIS-based noise mapping methods significantly expand the possibilities of visualizing and analyzing noise propagating from construction sites.[27,29] By combining noise measurements with spatial coordinates, it is possible to create color contour maps ("noise maps") that clearly identify areas of increased exposure and noise gradients around the construction site. The first applications of GIS in noise research have shown that mapping noise levels can help quantify the affected area and population with much higher resolution than discrete point measurements.[27] Modern research is developing this concept by using wireless sensor networks to continuously collect noise level data in construction areas. Low-cost digital noise level meters and IoT sensors can now be deployed around the workplace to transmit noise data in real time.[31] Mydlarz *et al*.[31] showed that a network of such sensors can reliably detect changes in urban noise at a fraction of the cost of traditional equipment. In the construction industry, researchers have developed real-time noise mapping systems that interpolate sensor readings to estimate noise levels in uncontrolled locations on the construction site.[32] For example, a recent work presented a system that optimizes the placement of sensors on a

construction site and uses spatial interpolation (for example, inverse distance weighting) to create almost instantaneous noise maps throughout the site. This approach achieved more than 96% accuracy in experimental tests, demonstrating that dynamic noise "heatmaps" are quite feasible for active work sites.[32] These real-time maps allow construction managers to see noise patterns changing as work progresses and quickly identify "hot spots" where noise levels need to be reduced. Innovative data processing techniques are also being applied to construction noise; one team has even explored the sonification of noise data, turning complex time histories of noise into audible feedback or warnings for intuitive monitoring.[11]

Overall, the combination of sensor data, GIS analytics, and advanced modeling propels construction noise management into a more proactive and informed epoch. Despite these achievements, significant gaps remain in the literature. Many field studies still rely on limited sampling or assume simplified propagation conditions (such as flat terrain and Euclidean distance) that may not reflect the true spatial scale of construction noise. In practice, sound travels over uneven landscapes and in various atmospheric conditions, factors that are often neglected in basic models. In addition, previous research has tended to focus on continuous or persistent sources of noise, such as car engines, while pulsed noises (such as pile driving, jackhammers, or blasting) have been studied less thoroughly and may behave differently when propagated and perceived. A recent systematic review notes the need for a more complete assessment of various types of noise on construction sites and more accurate forecasting tools for complex scenarios.[33] In particular, improving the modeling of pulsed construction noise and understanding its attenuation at a distance can help bridge the gap between simple theoretical expectations and actual measured noise levels on a construction site. Therefore, the purpose of this study is to study the patterns of propagation of pulsed noise from pile driving on a construction site. We combined field measurements with geospatial analysis to evaluate how pile-driving noise decreases with distance and evaluate the accuracy of the logarithmic distance model for this pulse source. By clarifying the distance-SPL dependence for pile-driving noise in real-world conditions, this work provides the necessary data to refine noise prediction models and identify effective noise-reduction strategies in construction environments. Ultimately, a better understanding of pulse noise propagation will help protect builders and residents of nearby areas from the dangers associated with high levels of construction noise.

2. Materials and methods

The study area used to investigate the outdoor noise distribution patterns is represented by the construction site in Astana, Kazakhstan (Fig. 1).[34] As shown in Fig. 1, the site is located in an open residential area with few existing buildings in the neighborhood to the south. The nearest residential building is at a distance of 60 m. The site area is roughly 20500 m^2 with extents from south to north and west to east of 208 and 193 m, respectively. On 11 June 2024, when the experiment was performed, pile driving was in progress at the site, which is also visible in the figure above. During the measurements (between 12:30 am and 1:00 am), the air temperature was 22.2-22.8 °C, and the relative humidity remained at 53%. Winds were predominantly from the north to north-northwest with average speeds of 5.8-7.2 m/s, and no significant gusts were recorded during this time. The sky was mostly cloudy, and the air pressure was stable at around 970.9 hPa.[35] The field experiment included noise measurements at various distances from the noise source (Fig. 2).

Fig. 1: Study area.[34]

Fig. 2 shows the construction site borders along with the noise source locations (*i.e.*, pile driving equipment) marked as a black circle and 4 measurement points marked as yellow rectangles positioned in a real geographical coordinate system WGS84 using latitude and longitude. These coordinates were recorded using a Global Navigation Satellite System (GNSS) GPS receiver and are as follows: Point 1 – 51.0816718, 71.49408131; Point 2 – 51.08174464, 71.49399804; Point 3 – 51.0817081, 71.49376516; and Point 4 – 51.0812561697826, 71.4933825046977.

The noise was recorded at the measurement points by calibrated UT352 sound level meters with an accuracy of 1.5 dB.[36] While the UT352's fast mode sampling rate is 125 microseconds (*i.e.*, 8 records per second), it does not automatically save the data in memory. Therefore, a smartphone's video camera was used to capture the data with 30 frames per second, as in the study of Imanov *et al.*,[12] so each numerical reading appears on screen for at least four video frames – more than enough to manually pause video and transcribe each 125 microseconds sample without ambiguity. The noise patterns were analyzed using a 5-second segment comprising 40 records per measurement point. For each record, we defined a logarithmic function of noise propagation (Eq. (1)) and calculated their empirical coefficients (a and b) and coefficients of determination (R^2) using a least

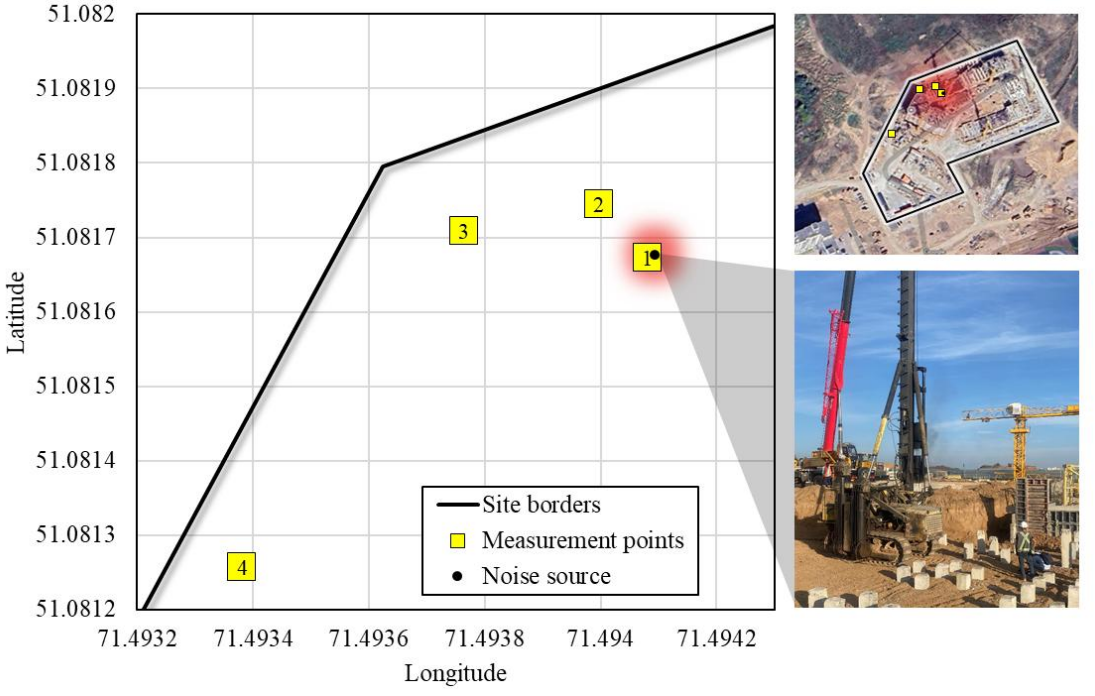

Fig. 2: Noise measurement setup.

squares method.[37]

$$L(d) = a \cdot ln(d) + b \quad (1)$$

where $L(d)$ is the sound pressure level; a and b are empirically determined coefficients; d is the distance from the noise source to the measurement point.

It is worth noting that, unlike Euclidean distance, the distance between the noise source and measurement points having geographical coordinates (latitude and longitude) was defined by a Haversine formula (Eq. (2)).[38]

$$d = 2R \cdot arcsin\left(\sqrt{sin^2\left(\frac{\Delta\varphi}{2}\right) + cos(\varphi_1) \cdot cos(\varphi_2) \cdot sin^2\left(\frac{\Delta\lambda}{2}\right)}\right) \quad (2)$$

where R is the radius of the Earth (6371 km); $\Delta\varphi$ and $\Delta\lambda$ are the differences in latitudes and longitudes of two points in radians, respectively. Although planar (Euclidean) distances computed by reprojecting WGS84 coordinates into a local metric system (UTM Zone 42N) differ from geodesic (Haversine) distances by less than 0.01 m (<0.015% of our 68.2 m maximum span), we employ the Haversine formula to compute distances directly from raw GNSS readings in WGS84. This avoids any projection-related distortions and future-proofs our workflow for larger construction sites, where ignoring Earth's curvature (even in its spherical approximation) can introduce non-negligible errors when spans extend into the hundreds of meters or kilometers.

To assess the logarithmic functions, we first estimated the SPL values for each record and distance using the coefficients a and b, and performed a correlation analysis to reveal the relationship between measured and estimated values of SPL. Then, a Scatter plot, Box plot, and Standard deviation analysis were performed to assess how well the functions approximate the real-world data. After that, we compared the logarithmic functions built from the extreme records (maximal and minimal) with those having the highest coefficient of determination (*i.e.*, the most reliable record). Here, as extremes, we took the records reflecting the maximal and minimal sums of SPLs within measured distances. Additionally, we made a comparison of the measured and estimated SPL values of the most reliable record to define the discrepancies and assess the accuracy of the noise propagation model. Finally, we estimated SPLs at all other surrounding distances from the source and built a 2D heatmap and 3D visualization of the impulse noise distribution.

3. Results and discussion

Fig. 3 shows the results of the noise measurements at 4 points at different distances from the source (*i.e.*, pile-driving equipment). The estimates given the coordinates (latitudes and longitudes) of the points using Eq. (2) yielded 1.0 m, 10.1 m, 23.2 m, and 68.2 m for points No. 1, 2, 3, and 4, respectively.

As shown in Fig. 3, the recorded noise levels of the pile-driving activity exhibit distinct patterns typical to impulse noise, characterized by periodic fluctuations in sound pressure levels. The data indicate an oscillation amplitude of roughly 17 dB, calculated as the difference between the highest peaks and the lowest valleys within the cycles of pile-driving noise. The length of these oscillations, determined by analyzing the distance between successive SPL peaks, averages around 8.3 records (1.0375 seconds), suggesting a temporal periodicity in the hammering impacts within a 5-second segment. The analysis of extremes reveals that the highest sum of SPLs

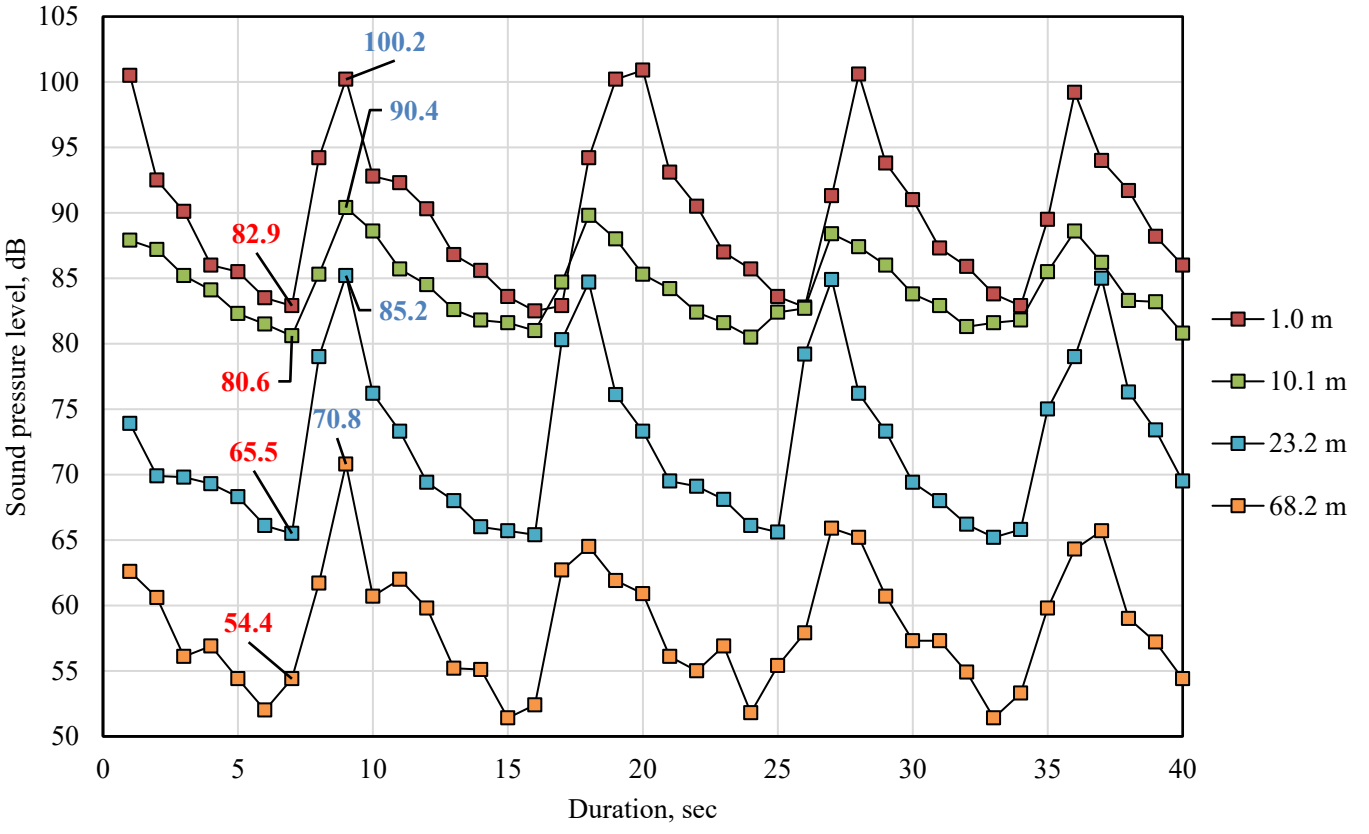

Fig. 3: SPLs at measured points.

occurs in record No. 9, where SPL values reach a peak of 100.2 dB at 1.0 m, 90.4 dB at 10.1 m, 85.2 dB at 23.2 m, and 80.8 dB at 68.2 m (marked blue in Fig. 3), indicating a strong impulse. In contrast, record No. 7 exhibits the lowest sum of SPLs, with values dropping to 82.9 dB, 80.6 dB, 65.5 dB, and 63.8 dB (marked green in Fig. 3) at the respective measurement points, marking a period of reduced impact force. The attenuation pattern seems to follow a logarithmic decay trend, which is consistent with theoretical models of spherical sound propagation, where SPLs decrease due to energy dissipation. Notably, at 23.2 m, certain peaks exceed 80 dB, which indicates that lower-frequency components of the pile-driving noise persist beyond expected levels, potentially due to ground-borne vibrations and secondary reflections. These findings confirm that pile-driving generates high-energy impulse noise with periodic fluctuations. This oscillation model is consistent with previous field observations of pulsed construction noise.

For example, Rönnberg *et al.*[11] reported characteristic periodic peaks in the time history of SPL at the construction site, and Imanov *et al.*[12] observed rapid fluctuations of 15-25 dB in pile driving noise, which closely coincides with the amplitude of fluctuations of ~17 dB observed in this case. High peak levels near the source (about 100 dB at a distance of 1 m) are also within the ranges noted in earlier studies: Chernuk *et al.*[9] recorded hammer blows during pile driving exceeding 110 dB at close range, and Shao *et al.*[10] found that the pulse noise from driven piles can remain at 100 dB even at a distance of 20 m. Although the peak we measured at a distance of 1 m is slightly lower than in some extreme cases,[9] maintaining the SPL level above 80 dB at a distance of 23 m repeats the far-reaching impact reported by Shao *et al.*,[10] confirming that pile driving produces intense, periodic noise pulses that carry significant energy over considerable distances.

Fig. 4 shows the *a* and *b* coefficients representing possible logarithmic functions of noise propagation of 40 records and their coefficients of determination R^2. Analysis of 40 logarithmic models fitted to the time and distance noise measurements shows a generally strong relationship between the coefficients *a* and *b* (Fig. 4(a)) and the quality of the fit, as measured by the coefficient of determination R^2 (Fig. 4(b)). Coefficients *a* range from approximately -9.38 to -3.99, with more negative values indicating sharper logarithmic noise attenuation, while coefficients *b* range from approximately 86.8 to 102.9, corresponding to baseline noise levels. An inverse correlation can be seen: steeper slopes (more negative *a*) correspond to higher crossings (*b*), indicating that louder noise sources tend to attenuate faster. The R^2 values confirm the fit of the logarithmic model for most intervals: 31 of the 40 records (77.5%) have R^2 values greater than 0.80, including several high-impact values such as 0.97, 0.96, and 0.94. However, three intervals have noticeably lower R^2 values of 0.50, 0.55, and 0.66, indicating that the model poorly represents the noise behavior in these cases, possibly due to environmental interference or measurement anomalies.

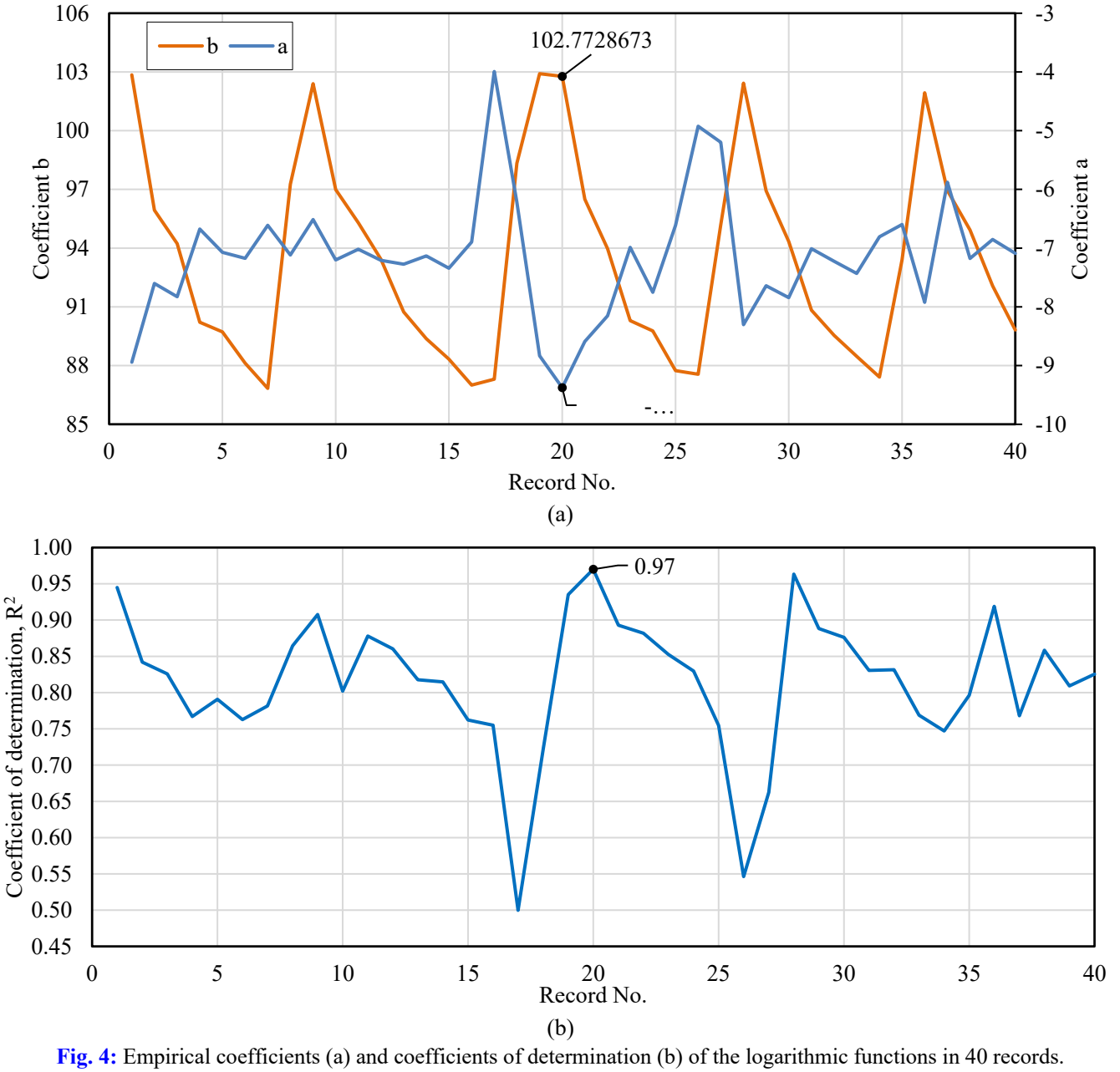

Fig. 4: Empirical coefficients (a) and coefficients of determination (b) of the logarithmic functions in 40 records.

Overall, the logarithmic function appears to be an acceptable and consistent approximation for modeling noise attenuation.

Moreover, considering the highest R^2 of 0.97 from a given array on record No. 20, the respective values of empirical coefficients *a* and *b* (-9.376058998 and 102.7728673) shown in Fig. 4(a) could form a logarithmic function enabling a highly reliable approximation of the impulse noise propagation in this setup (i.e., optimal throughout the records). These coefficient values can be compared with typical attenuation characteristics given in the literature. Under ideal conditions of a free field, the sound pressure level decreases by about 6 dB by doubling the distance (equivalent to $a \approx 20$ in the logarithmic model).[22] The fact that our empirical values of *a* (from 4 to 9) are significantly lower than the ideal value of 20 indicates a slower rate of attenuation in the real world, probably due to reflection from the ground or atmospheric factors. Similar empirical modeling conducted by Wu *et al.*[22] for noise on a construction site also showed that a simple logarithmic decay ensures a good match (high R^2) to the measured data, even despite deviations in certain intervals. Our observation that most records give $R^2 > 0.8$, and only a few of them show poor compliance, is consistent with the conclusions of Wu *et al.*[22] that logarithmic regressions usually reflect noise attenuation well at a distance but may fail under abnormal environmental conditions.

Fig. 5 shows the values of SPL estimated by respective logarithmic functions along with the measured values of SPL at various distances. In Fig. 5, a comparison of the measured (M) and estimated (E) SPL values at four distances (1.0 m, 10.1 m, 23.2 m, and 68.2 m) using Eq. (1) and coefficients from Fig. 4(a) shows that the models provide fairly accurate

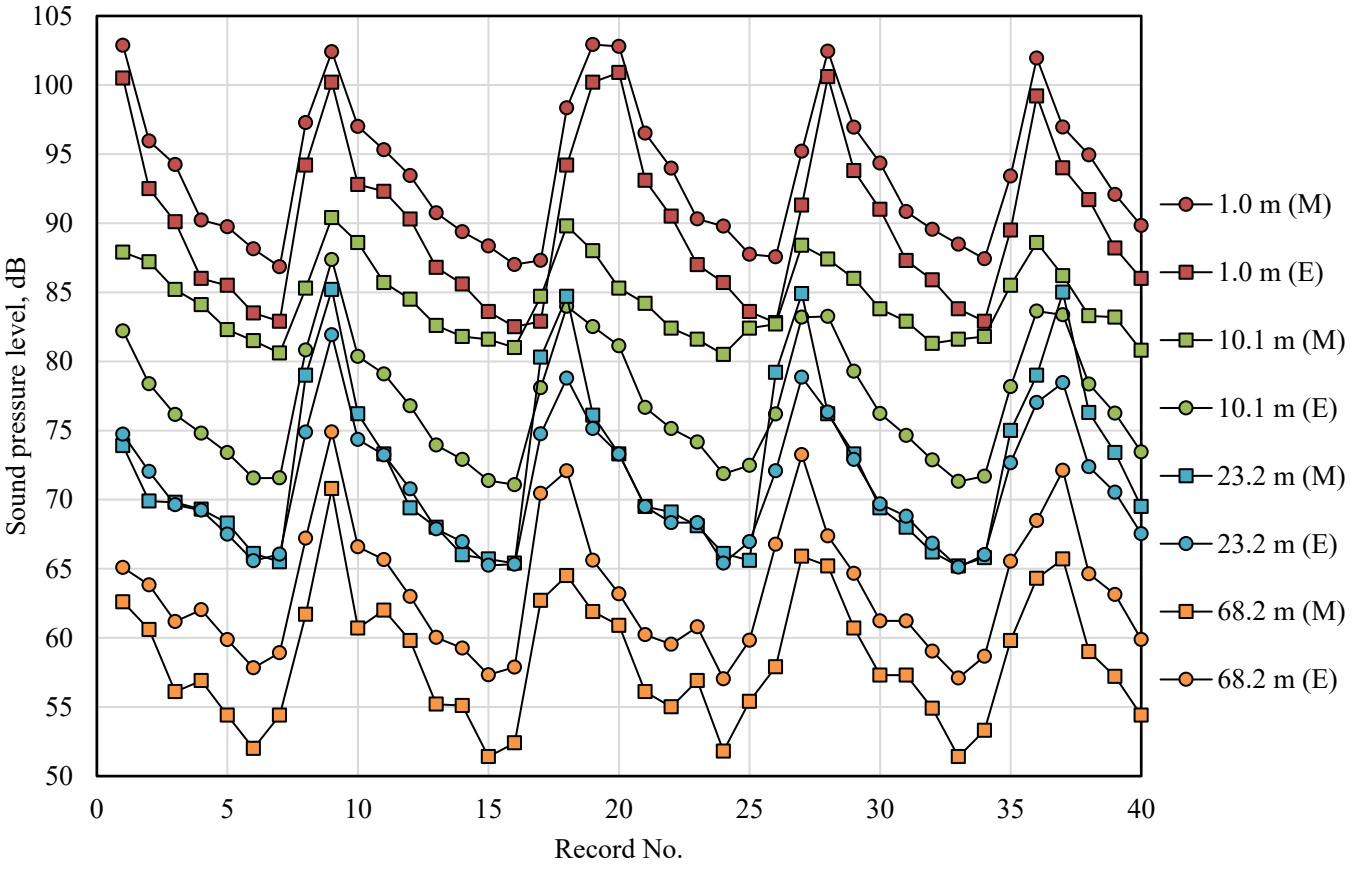

Fig. 5: Comparison of measured (M) and estimated (E) values of SPL.

forecasts with some variation depending on the distance. Thus, at a distance of 1.0 m, the estimated SPL values are slightly higher than the measured ones, with an average overestimation of about +3.63 dB. At a distance of 10.1 m, the estimated values are lower than the actual measurements, on average by -7.32 dB. At a distance of 23.2 m, the estimated values are closer, but the SPL is still often underestimated, with an average deviation of about -1.23 dB. At the farthest point, 68.2 m, the models slightly overestimate the value, with an average deviation of +4.92 dB. These results show that logarithmic models reflect the general trend of attenuation well, especially at short and long distances, but tend to underestimate SPL values at intermediate distances. Such discrepancies, depending on the distance, are consistent with observations obtained in previous studies using similar models. For example, Wu *et al.*[22] noted that although the logarithmic distance model reflects the overall noise attenuation, it may not perfectly predict levels at each interval, probably due to localized effects, which in our case is obvious at a distance of 10.1 m, where an additional deviation of -7 dB occurs. The ground reflections from the soil interface and minor obstructions likely contribute to the underestimation at ~10 m. Incorporating a reflection-correction term or explicitly modeling obstacle geometry could improve model performance, which may be addressed in future work. Relatively small deviations at 1.0 m and 68.2 m (within ~3-5 dB) indicate the strength of the model at extreme distances, while underestimating the average range indicates the limitations of the one-parameter approach. This pattern highlights why recent researchers are exploring more sophisticated forecasting methods.[39,40] For example, Ooi *et al.*[23] have developed a deep learning model to account for additional factors (type of equipment, barriers, *etc.*) and improve accuracy over various distances. Our results also indicate that taking into account such factors can reduce the error over intermediate distances, although even a simple logarithmic approach demonstrates a fairly high accuracy in accordance with previous empirical models.[22]

Fig. 6 shows how the correlation between the measured and estimated values of SPL changes as distance increases. Correlation analysis in Fig. 6 above shows consistently strong agreement between the measured and estimated SPL values at all distances, with correlation factors (r) from 0.94 to 0.997, following a logarithmic trend. The resulting equation "y = -0.011ln(x)+0.9873" reflects a gradual decrease in correlation with increasing distance, and the coefficient of determination $R^2 = 0.636$ indicates its moderate fit. The strongest correlation is observed at a distance of 1.0 m ($r = 0.997$), which confirms the excellent performance of the model near the source. A noticeable dip appears at a distance of 10.1 m ($r = 0.940$), indicating a decrease in accuracy at this average level. Interestingly, the correlations at distances of 23.2 m (r =

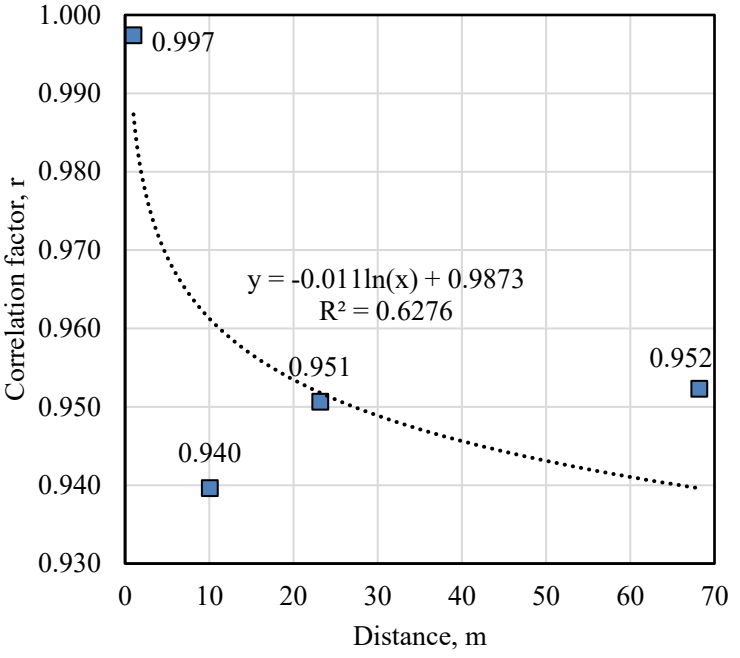

Fig. 6: Correlation analysis.

0.951) and 68.2 m (r = 0.952) remain relatively stable and stronger than expected, which means that the model remains reliable over long distances. This logarithmic trend line can be used to approximate correlation over unmeasured distances and to identify potential areas where model adjustments may be useful. The high correlation coefficients ($r \geq 0.94$ for all points) correspond to the good match achieved by simple attenuation models in other field studies. Wu *et al*.[22] also reported a strong correlation (and high R^2 values) when fitting logarithmic attenuation to noise measurements, indicating that the fundamental relationship between distance and noise level is stable under practical conditions. A slight drop in correlation at an average distance (about 10 m) reflects minor discrepancies noted in the analysis of Fig. 5 and suggests that certain ranges of distances may introduce anomalies, a phenomenon that was also hinted at in a previous empirical study, where some average distance data did not fully match the logarithmic trend. Nevertheless, the overall strong correlation confirms that the model's predictions are closely related to the actual measurements, as it was found in previous studies in a relatively open area.[22]

Fig. 7 shows a Scatter plot, Box plot, and Standard deviation analysis of the measured and estimated values of SPL. The Scatter plot and Box plot in Fig. 7 jointly reveal the performance of the logarithmic model in estimating SPLs over four distances of 1.0 m, 10.1 m, 23.2 m, and 68.2 m based on 160 readings. The Scatter plot in Fig. 7(a) shows a strong positive correlation between measured and estimated SPLs, with points consistently following the diagonal (red dots) at 1.0 m and 23.2 m, indicating high model accuracy at these distances. At 10.1 m, however, estimated values systematically fall below the diagonal, reflecting an underestimation, while the points at 68.2 M are slightly above the diagonal, showing an overestimation observed in Fig. 5. The Box plot in Fig. 7(b) confirms these trends: at 1.0 m, the median estimated SPL is about 3.6 dB higher than the measured median (93.4 dB vs. 89.8 dB); at 10.1 m, the estimated median drops to 76.2 dB, while the measured median is 83.9 dB; at 23.2 m, the medians are closely aligned (70.1 dB estimated vs. 69.7 dB measured); and at 68.2 m, the estimated median is 62.5 dB compared to the measured 57.3 dB. The interquartile ranges (IQR) of estimated values falling between 5.8 dB and 7.4 dB are rather lower than measured ones, amounting to 4.2-8.2 dB, reflecting a single difference of roughly 2.8 dB at the distance of 10.1 m. Overall, the model performs best at 1.0 m and 23.2 m, underestimates at 10.1 m, and slightly overestimates at 68.2 m, confirming its overall reliability with distance-specific deviations.

The standard deviation (STDV) curves show that the measured SPL values vary more strongly at different distances, reaching 6.2 dB at the distance of 23.2 m, while the estimated SPL values remain more constant, ranging from 4.4 to 5.1 dB. The model underestimates the variability of the real world, especially at a distance of 23.2 m, where the STDV difference is greatest (6.2 versus 4.5 dB). At the distance of 10.1 m, the measured STDV is the lowest (2.8 dB), and model one is higher (4.4 dB), which may indicate the presence of additional noise. These results show that although the central trend is well captured, the model smooths out some of the variability inherent in the measured data. This behavior is usually noted in noise modeling studies. Thus, the empirical attenuation model by Wu *et al*.,[22] for example, gave a relatively narrow predicted range compared to the fluctuations observed in real field measurements. In our case, the calculated SPL values obtained using the model have a smaller spread (lower IQR and STDV) than the measured SPL, which indicates that

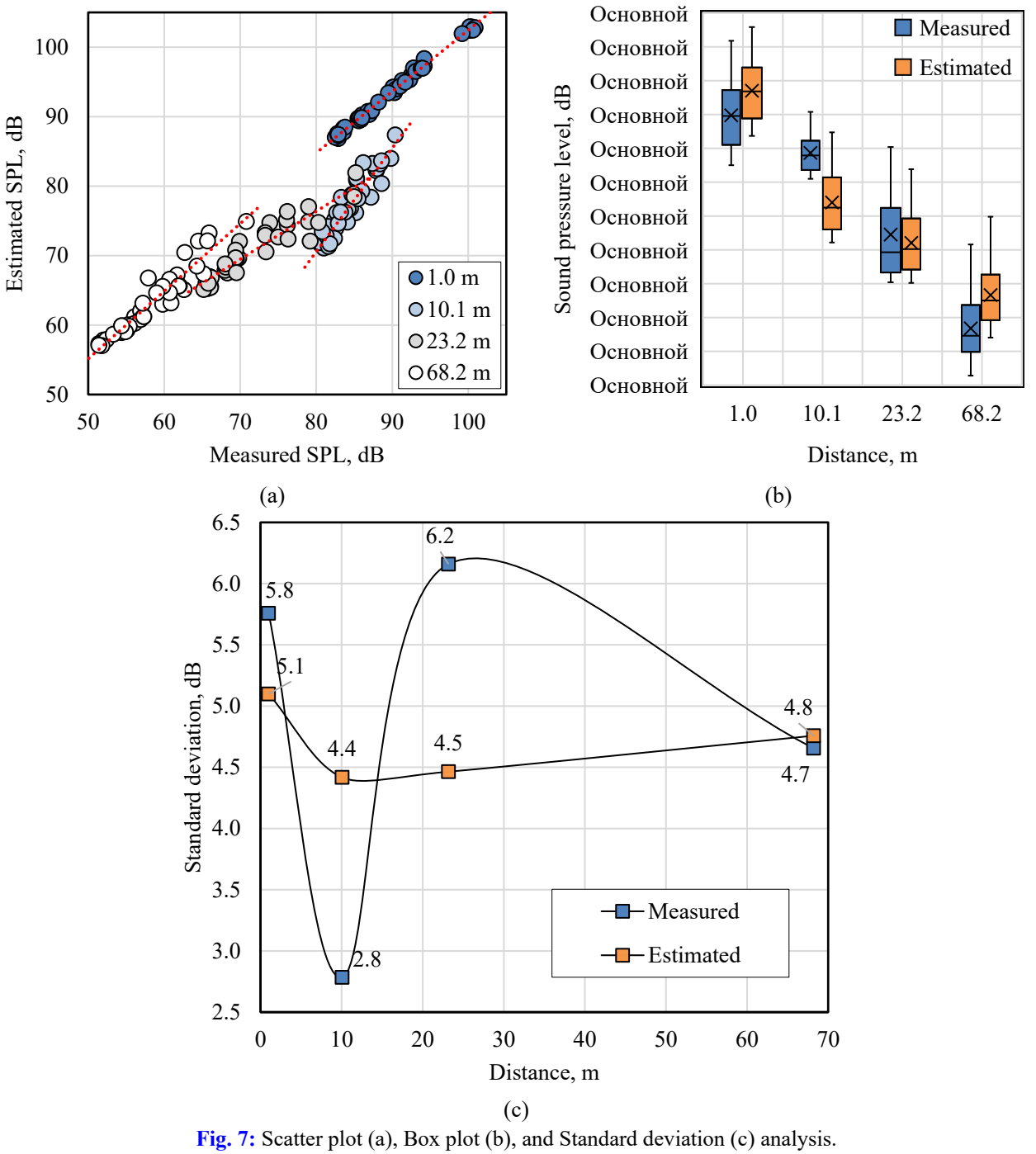

Fig. 7: Scatter plot (a), Box plot (b), and Standard deviation (c) analysis.

the model does not fully account for transient deviations that may be caused by environmental or operational variability. This is consistent with the understanding that single-parameter models prone to average micro-scale influences (wind gusts, short-term changes in machine orientation, etc.), which leads to more uniform and smoother forecasts.[22] Despite this, the main patterns of underestimation in the middle range (i.e., distance) and minor overestimation in the long range reflect the systematic errors identified earlier, confirming that the reliability of the model as a whole is relatively high, but it may miss subtle fluctuations that could be detected by more advanced or multifactorial models.[23]

Fig. 8 shows the comparison of logarithmic functions based on the extremes identified in records No. 9 and 7 (Fig. 3), and values of record No. 20 yielding the highest R^2 (Fig. 4(b)). The diagram in Fig. 8 presents three models describing noise propagation (optimal, maximal, and minimal), each plotted against distance with their corresponding logarithmic equations and R^2. The maximal curve (along green circles) is expressed as $y = -6.513\ln(x)+102.4$ with $R^2 = 0.9077$, representing the typical or most probable noise decay scenario under loud conditions (peak amplitudes of SPL). The minimal curve (along blue circles) has the equation $y = -6.61\ln(x)+86.835$ and a lower $R^2 = 0.7816$, indicating greater

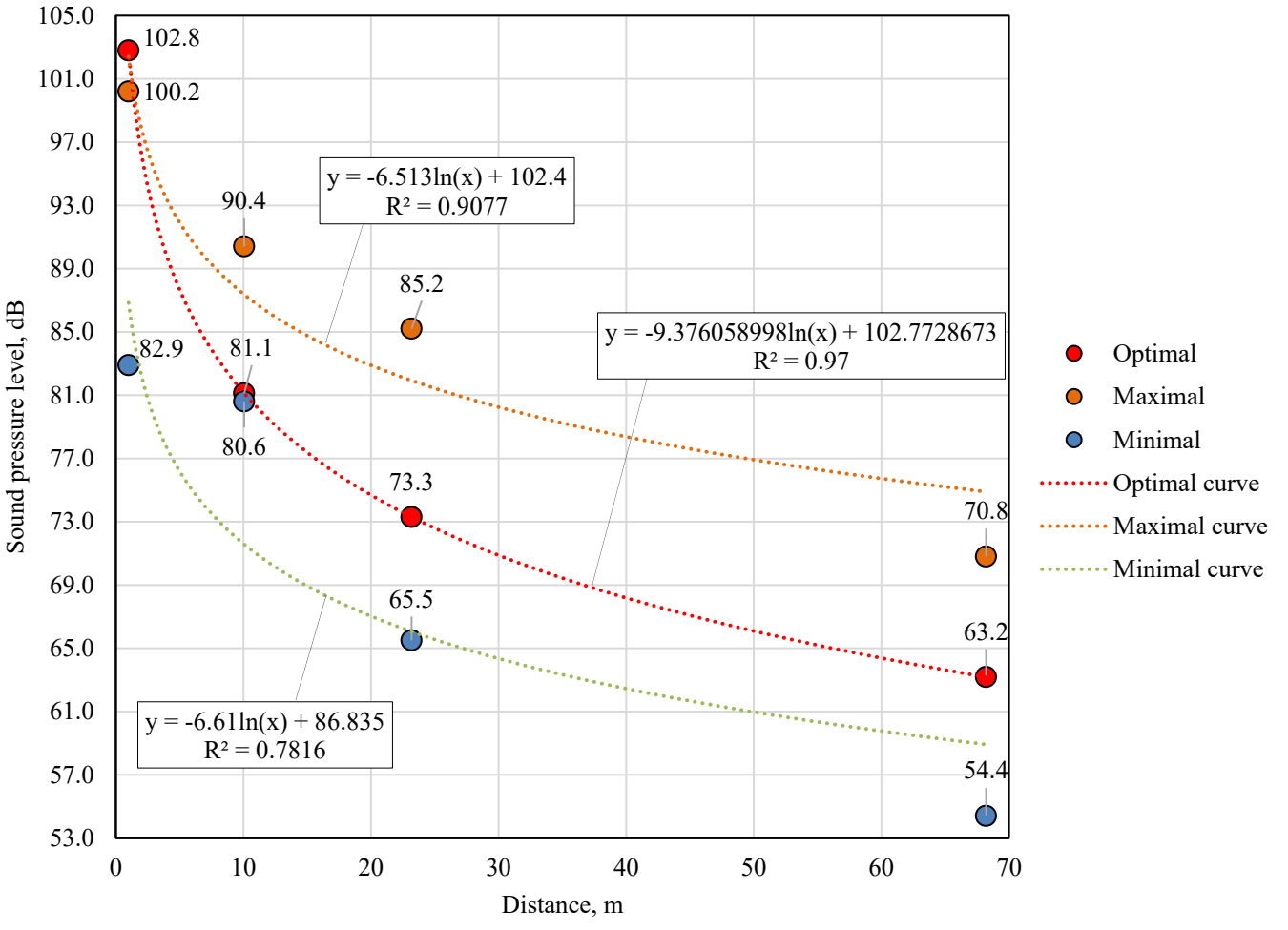

Fig. 8: Models of pile-driving noise propagation at peaks and dips.

variability and weaker model fit in the quietest conditions (dip amplitudes of SPL). In contrast, the optimal curve (along red circles) follows y = -9.376058998ln(x)+102.7728673 with a strong $R^2 = 0.97$, reflecting the steepest decay under moderate conditions. All three curves confirm that the noise level decreases logarithmically with increasing distance both at peaks and dips, while the disparity between the actual values and forecasts emphasizes the effect of changes in the environment or source level on the propagation pattern. This set of models illustrates how different noise emission scenarios (loud peaks versus quiet intervals) can change the apparent attenuation rate, which has also been noted in previous studies. The overall logarithmic decrease in SPL with distance is expected from the point of view of fundamental acoustics and corresponds to the standard propagation laws (approximately 6 dB of loss per doubling of distance in a free field).[25] However, the variation of slope (a) between the maximum, minimum, and optimal cases suggests that the real factors (for example, different hammer impact energy or background noise) affect the effective attenuation rate.

A similar variability was observed by Wu *et al.*,[22] who reported that the attenuation curves may differ under different noise conditions, although the general logarithmic form remains correct. In our results, a steeper attenuation of the optimal curve indicates that with moderate, constant hammer impact, noise decreases faster, while more gentle slopes in peak and dip cases mean steady noise levels, possibly due to reflective or surface contributions when the source is very loud or at low background moments. These differences are consistent with the idea that environmental conditions and fluctuations in the intensity of the source can cause deviations in the propagation of noise. This effect is also hinted at by field tests of noise from pile driving in various operating modes.[10] Nevertheless, the logarithmic model is preserved in all scenarios, which confirms the stability of this attenuation model.[25] even if the exact coefficients vary depending on the conditions.

Fig. 9 uses the noise propagation function reflecting the optimal curve in Fig. 8 to estimate the SPL values throughout the whole study area (construction site from Figs. 1 and 2) and shows them as a heatmap. The heatmap in Fig. 9 above visually represents the distribution of noise levels across the study area (construction site), with higher SPL values concentrated near the noise source (pile-driving equipment), decreasing outward, and ranging from 100.8 dB to 55.4 dB, respectively. High-risk zones, where SPL is 85–100 dB, are circled using a dashed line, indicating areas requiring hearing protection. Such levels of noise may cause some

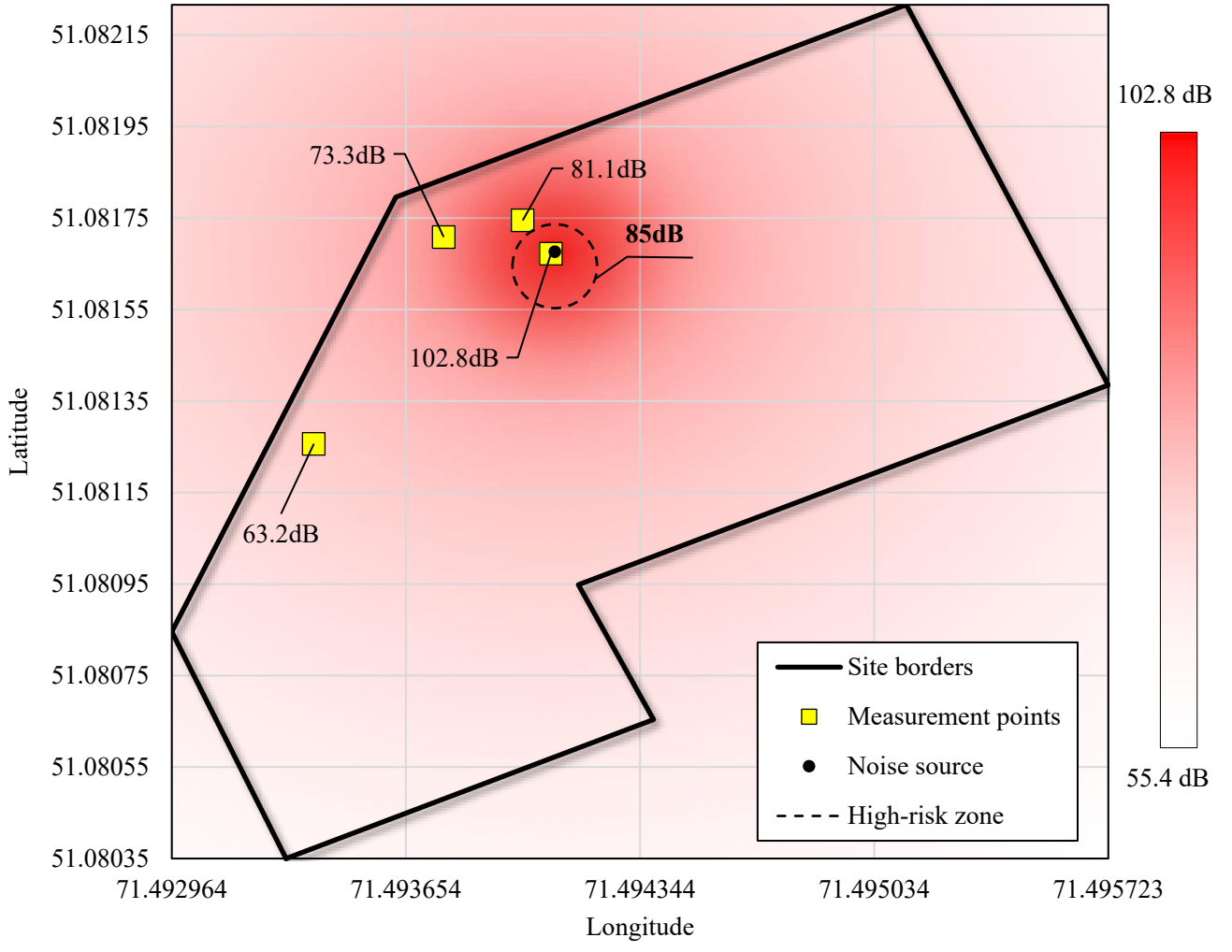

Fig. 9: Heatmap of pile-driving noise propagation.

inconvenience to the workers on the site, suggesting the use of protective headphones. Such levels of noise do not reach the inhabitants of the nearest residential building 60 meters from a construction site's borders or 190 m from the noise source (Fig. 1), since the estimated SPL at this location is 53.6 dB. Notably, the calculated SPL values at the measurement points (marked in yellow) are slightly different from the actual measurements. This suggests a rationale for discrepancy analysis (Fig. 10) to reveal the relative accuracy of the noise propagation model. The spatial propagation shown in Fig. 9 is comparable to the results of other studies on mapping construction noise. Li *et al.*,[32] for example, compiled real-time noise maps for active construction sites and similarly observed concentric zones of high SPL levels around the noise source, which disappeared with distance, highlighting the places where workers are most at risk. On our heat map, the area exceeding 85 dB near the piling unit is of particular concern since it is known that prolonged exposure to noise above ~85 dB can lead to hearing damage.[15] This is consistent with epidemiological data showing high levels of hearing loss among construction workers who are regularly exposed to such levels and field studies on Beijing construction sites, where heavy equipment often brought noise to the construction site beyond safe limits.[15,18] The allocation of an area of 85-100 dB confirms these observations and highlights the need for hearing protection in these areas. On the positive side, our model shows that the noise dissipates enough to save residents of nearby areas from dangerous effects, remaining at the level of 53-54 dB at a distance of 190 m from the source. This contrasts with scenarios such as the construction of oil and gas wells, studied by Blair *et al.*,[8] where construction noise increased the noise level in a populated area to more dangerous thresholds. In our case, a rapid decrease to a safe level on the perimeter of residential areas indicates that the open layout and distance are sufficient to protect the public, which corresponds to the idea that attenuation of sound by 100 m can reduce the construction noise to the level of the environment.[8] In general, the spatial distribution on the heatmap corresponds to the expected distribution in an open space and corresponds to the documented schemes of construction noise exposure zones.[18,32]

Fig. 10 compares measured and estimated SPLs at four distances and quantifies the model's accuracy using percent error. The model demonstrates excellent accuracy at a distance

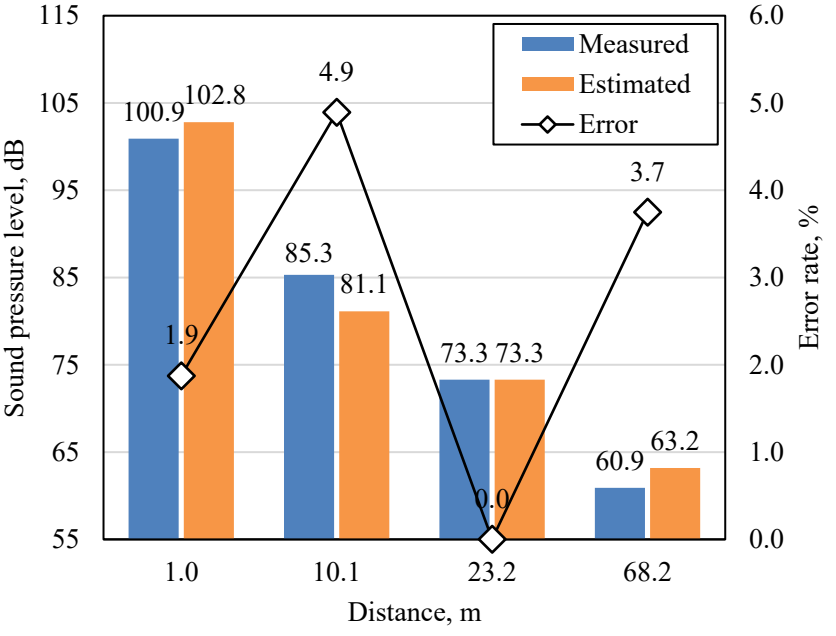

Fig. 10: Discrepancy analysis.

of 23.2 m with no error, where the measured and estimated SPLs match exactly at 73.3 dB. At a distance of 1.0 m, the error is small (1.9%), where the estimated SPL is slightly higher than the measured value (102.8 vs. 100.9 dB). The largest deviation is observed at a distance of 10.1 m, where the model underestimates the noise level by 4.9% (81.1 vs. 85.3 dB). At a distance of 68.2 m, the error is 3.7%, which also indicates a slight overestimation. Overall, the model demonstrates high accuracy, especially at medium distances, with an average error across all points of only 2.6%, confirming its reliability in estimating noise propagation. This level of accuracy (with errors usually less than 5%) is comparable to similar models reported in the literature. In a study by Wu *et al*.[22] on a different external noise environment, the logarithmic model corresponded highly, assuming only minor percentage differences between the observed and predicted levels. Our conclusion that the model is practically accurate at one distance (23.2 m) and with an accuracy of up to several percent at others reflects the view that simple logarithmic distance models can be quite effective for outdoor conditions.[22] Although more complex models can further improve the accuracy of the forecast,[23] the low average error of 2.6% in this case underlines that the fundamental logarithmic approach can give reliable results. This is consistent with previous studies using basic attenuation formulas, achieving small deviations when environmental factors were sufficiently constant.[22] Thus, the analysis of discrepancies confirms that the predictive power of our model is comparable to the results obtained in earlier field noise estimates, which confirms its use for practical forecasting of construction noise. Although our measurement timeframe was very short (only five seconds between 12:30 PM and 1:00 PM), moderate meteorological factors could have contributed to the remaining deviations. Historical data for Astana from June 11, 2024 show an air temperature of ~ 22.5 °C,[35] a relative humidity of about 53%, north-northwesterly winds of ~ 6.5 m/s, and a constant air pressure of ~ 970.9 hPa. Such wind speeds and directions may distort the sound propagation asymmetrically, even over a few seconds, and slightly shift the sound pressure measurements, especially in intermediate ranges. Future work should combine high-speed acoustic sampling with on-site anemometry and thermometry to attempt isolating and correcting for these effects.

Fig. 11 shows a 3D visualization of the spherical distribution of impulse noise sourced by pile-driving activity. The surface diagram in Fig. 11 provides a spatial visualization of the propagation of noise over a study area with the resolution of 1×1 m^2, effectively simulating how sound pressure levels decrease from a central source. The highest SPL level, exceeding 100 dB (marked red), is concentrated at the peak point – directly above the noise source – and decreases rapidly with radial distance, forming concentric intensity reduction zones. At distances of 1-11 m, the SPL falls within 80-100 dB (marked orange). The next zone is represented by the distances of 12-96 m, with SPL falling within 60-80 dB (marked blue). At farther distances, SPL continues to decrease toward the periphery, dropping below 60 dB (marked green). The smooth gradient and symmetrical shape indicate a uniform spread in an open space with minimal obstacles or a shift in direction. This visualization clearly illustrates the logarithmic nature of sound attenuation and may serve as a practical tool for assessing noise impacts in spatial areas during noise control. The concentric, spherical distribution observed in this case is fully consistent with theoretical expectations and has been demonstrated in other works on noise mapping. According to the ISO 9613-2 standard for the propagation of sound outdoors,[25] sound emitted by a point source in a free field creates almost circular

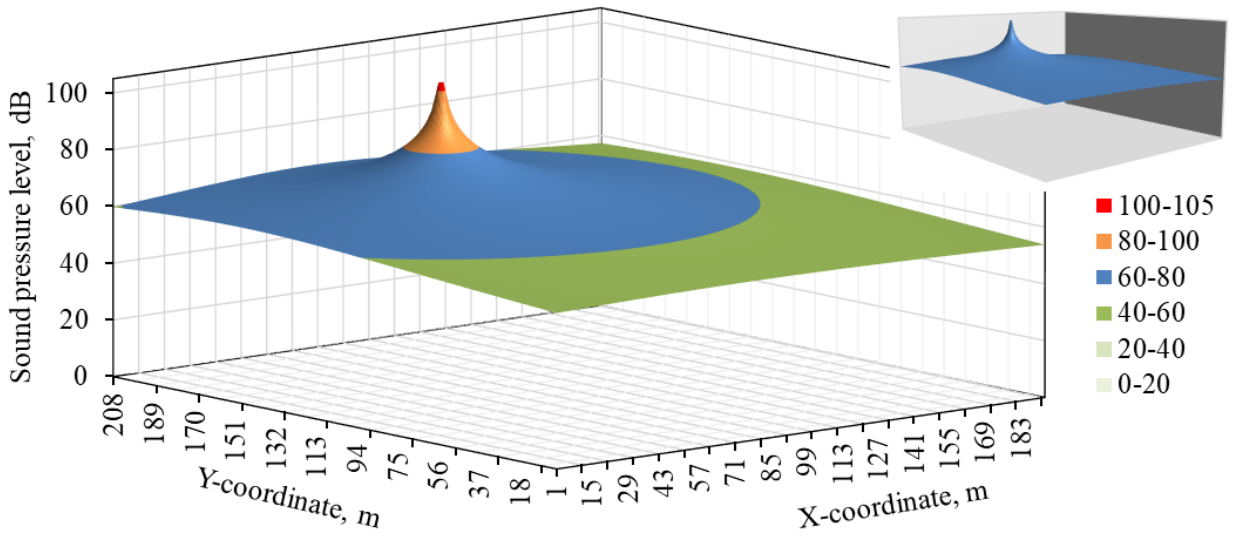

Fig. 11: 3D visualization of pile-driving noise propagation.

(or spherical in 3D) contours of equal level, as shown in Fig. 11. Empirical studies on mapping construction sites, such as the work of Lee *et al.*,[32] gave similar visual patterns. The noise intensity is maximum at the source and attenuates relatively evenly in the absence of obstacles. The core of 80-100 dB in our 3D model and the successive rings of 60-80 dB and <60 dB resemble the noise zones described by Lee *et al.*[32] in a real construction scenario, which confirms the commonality of these zones for heavy machinery noise. The symmetry and smooth attenuation additionally confirm that there are no large reflective structures or relief anomalies on the site that affect noise propagation, which corresponds to the assumptions of many noise models and instruments that simulate sound propagation in open areas.[26] From a practical perspective, the close agreement between our visualization and known propagation characteristics means that the model can be useful for planners: it confirms that the high-noise area is confined to the source and that standard recommendations for protective distance (*e.g.*, for safe exposure) are applicable.[25,32] Thus, this kind of 3D noise map is not only consistent with the literature results, but also provides an intuitive means to assess and compare noise impact areas, supporting more informed noise mitigation strategies recommended in recent studies.[32,33]

4. Conclusion

It has been confirmed that pile driving on construction sites generates high-intensity pulsed noise characterized by repetitive peaks and dips. In our field measurements, sound pressure levels fluctuated by about 17 dB over one-second intervals, highlighting the cyclical effects of hammer blows. The attenuation of these noise levels with distance was well described by the logarithmic attenuation model. Most of the recorded intervals showed a strong degree of compliance for this attenuation model (the coefficients of determination of R^2 are higher than 0.8 in almost 78% of cases), and the optimal model reached R^2 0.97. This indicates that, under typical conditions, a simple logarithmic function can effectively capture a decrease in SPL from a pulsed source of construction noise.

The model's predictions closely matched the measured values at all measured locations, with an average discrepancy of only a few decibels (approximately 2-3% error). We observed small shifts depending on the distance: at an intermediate distance (~10 m from the source), the model tended to underestimate the noise level, while it slightly overestimated it at the furthest measured point (~68 m). Despite these minor deviations, the overall trend and correlation between measured and predicted sound pressure levels remained consistently strong, confirming the reliability of logarithmic attenuation modeling for this context.

The integration of this logarithmic model with geospatial analysis provides clear practical ideas for managing construction noise. The generated noise maps (2D heatmap and 3D visualization) illustrate the concentric decline of SPL around the pile-driving site. A high-risk area was identified near the hammer, where SPL ranges from about 85 dB to 100 dB. Within this immediate area (on the order of the first few tens of meters), workers will be exposed to levels that require hearing protection and other safety measures. Outside of this area, noise levels are rapidly reduced to safer values.

At the boundary of the site (~60 m from the source in our study), the predicted SPL drops to about 55-60 dB. This indicates that the noise impact on the surrounding community (for example, residents of the nearest building at a distance of about 190 m) remains well below harmful or destructive thresholds. These results are translated into practical recommendations. Thus, construction managers can use such modeling to identify areas of "noisy work" where protective equipment is required and to ensure that noise around the perimeter does not exceed regulatory limits. Overall, the study shows that combining empirical field data with logarithmic

propagation modeling and spatial visualization is an effective strategy for predicting noise propagation. This comprehensive approach helps in establishing evidence-based protection zones on construction sites, thereby protecting workers' hearing and minimizing the impact of noise on the nearby population. Extending this framework with a network of low-cost acoustic sensors feeding real-time sound-level data into a GIS-based dashboard would allow dynamic adjustment of these zones and automated alerts when thresholds are exceeded. This combined methodology offers a robust, academically grounded model for both static planning and adaptive, real-time noise control on construction sites.

Our analysis is limited by the small number of measurement points and the absence of real-time meteorological monitoring during pile driving. The ground impedance and mapping of on-site obstacles were also not considered. Therefore, future research should deploy a denser sensor network, record environmental parameters (wind speed/direction, temperature, humidity) in parallel with acoustic sampling, integrate ground and obstacles reflection factor, and explore more sophisticated propagation models to further improve predictive accuracy.

Acknowledgments

This research was funded by the Science Committee of the Ministry of Science and Higher Education of the Republic of Kazakhstan (Grant No. AP19674718).

Conflict of Interest

There is no conflict of interest.

Supporting Information

Not applicable.

References

[1] R. Chepesiuk, Decibel hell: the effects of living in a noisy world, *Environmental Health Perspectives*, 2005, **113**, A34-A41, doi: 10.1289/ehp.113-a34.

[2] M. Basner, W. Babisch, A. Davis, M. Brink, C. Clark, S. Janssen, S. Stansfeld, Auditory and non-auditory effects of noise on health, *The Lancet*, 2014, **383**, 1325-1332, doi: 10.1016/S0140-6736(13)61613-X.

[3] W. Babisch, Road traffic noise and cardiovascular risk, *Noise & Health*, 2008, **10**, 27-33, doi: 10.4103/1463-1741.39005.

[4] S. A. Stansfeld, M. P. Matheson, Noise pollution: non-auditory effects on health, *British Medical Bulletin*, 2003, **68**, 243-257, doi: 10.1093/bmb/ldg033.

[5] A. Can, A. L'Hostis, P. Aumond, D. Botteldooren, M. C. Coelho, C. Guarnaccia, J. Kang, The future of urban sound environments: Impacting mobility trends and insights for noise assessment and mitigation, *Applied Acoustics*, 2020, **170**, 107518, doi: 10.1016/j.apacoust.2020.107518.

[6] C. Zou, R. Zhu, Z. Tao, D. Ouyang, Y. Chen, Evaluation of building construction-induced noise and vibration impact on residents, *Sustainability*, 2020, **12**, 1579, doi: 10.3390/su12041579.

[7] B. Barkokébas Jr, B. M. Vasconcelos, E. M. G. Lago, A. F. P. Alcoforador, Analysis of noise on construction sites of high-rise buildings, *Work*, 2012, **41**, 2982-2990, doi: 10.3233/WOR-2012-0553-2982.

[8] B. D. Blair, S. Brindley, E. Dinkeloo, L. M. McKenzie, J. L. Adgate, Residential noise from nearby oil and gas well construction and drilling, *Journal of Exposure Science & Environmental Epidemiology*, 2018, **28**, 538-547, doi: 10.1038/s41370-018-0039-8.

[9] V. P. Chernuk, V. P. Shcherbach, E. I. Shlyahova, Ecological features of pile works in construction, *Vestnik of Brest State Technical University*, 2021, **136**, 82-84, doi: 10.36773/1818-1112-2021-126-3-82-84.

[10] F. Shao, Y. Deng, S. Chen, R. Zheng, R. Zhang, Field test study on construction disturbances of driven pile and PGP pile, *Applied Sciences*, 2023, **13**, 11887, doi: 10.3390/app132111887.

[11] N. Rönnberg, R. Ringdahl, A. Fredriksson, Measurement and sonification of construction site noise and particle pollution data, *Smart and Sustainable Built Environment*, 2023, **12**, 742-764, doi: 10.1108/sasbe-11-2021-0189.

[12] A. Imanov, A. Kozhas, A. Mukhamejanova, A. Nazarova, D. Kazhimkanuly, Experimental study of sound wave propagation patterns, *Technobius*, 2024, **4**, 57, doi: 10.54355/tbus/4.2.2024.0057.

[13] X. Yang, Y. Wang, R. Zhang, Y. Zhang, Physical and psychoacoustic characteristics of typical noise on construction site: "how does noise impact construction workers' experience?", *Frontiers in Psychology*, 2021, **12**, 707868, doi: 10.3389/fpsyg.2021.707868.

[14] A. Dzhambov, D. Dimitrova, Occupational noise exposure and the risk for work-related injury: a systematic review and meta-analysis, *Annals of Work Exposures and Health*, 2017, **61**, 1037-1053, doi: 10.1093/annweh/wxx078.

[15] E. A. Masterson, J. A. Deddens, C. L. Themann, S. Bertke, G. M. Calvert, Trends in worker hearing loss by industry sector, 1981–2010, *American Journal of Industrial Medicine*, 2015, **58**, 392-401, doi: 10.1002/ajim.22429.

[16] R. Neitzel, N. Seixas, The effectiveness of hearing protection among construction workers, *Journal of Occupational and Environmental Hygiene*, 2005, **2**, 227-238, doi: 10.1080/15459620590932154.

[17] S. A. Ali, A case study of construction noise exposure for preserving worker's hearing in Egypt, *Acoustical Science and Technology*, 2011, **32**, 211-215, doi: 10.1250/ast.32.211.

[18] J. Xiao, X. Li, Z. Zhang, DALY-based health risk assessment of construction noise in Beijing, China, *International Journal of Environmental Research and Public Health*, 2016, **13**, 1045, doi: 10.3390/ijerph13111045.

[19] M. Nurtas, Z. Baishemirov, Y. Aizhan, A. Aizhan, 2-D Finite Element method using "eScript" for acoustic wave propagation, *Proceedings of the 6th International Conference on Engineering & MIS 2020*, Almaty, Kazakhstan, ACM, 2020, 1-7, doi: 10.1145/3410352.3410774.

[20] M. Nurtas, Y. Aizhan, A. Aizhan, Using of Machine Learning algorithm and Spectral method for simulation of Nonlinear Wave Equation, *Proceedings of the 6th International Conference on Engineering & MIS 2020*, Almaty, Kazakhstan, ACM, 2020, 1-6, doi: 10.1145/3410352.3410778.
[21] M. Nurtas, Z. Baishemirov, S. Alpar, F. Tokmukhamedova, Numerical simulation of wave propagation in mixed porous media using finite element method, *Journal of Theoretical and Applied Information Technology*, 2021, **99**, 4163-4172.
[22] Y. Wu, J. Kang, W. Zheng, Acoustic environment research of railway station in China, *Energy Procedia*, 2018, **153**, 353-358, doi: 10.1016/j.egypro.2018.10.038.
[23] W. C. Ooi, M. H. Lim, Y. L. Lee, Development of stochastic deep learning model for the prediction of construction noise, *Ain Shams Engineering Journal*, 2024, **15**, 102592, doi: 10.1016/j.asej.2023.102592.
[24] A. H. Boussabaine, Artificial neural networks for predicting noise from construction sites, *Building Acoustics*, 1997, **4**, 211-221, doi: 10.1177/1351010x9700400304.
[25] ISO, ISO 9613-2:2024 Acoustics – Attenuation of sound during propagation outdoors, Part 2: Engineering method for the prediction of sound pressure levels outdoors, International Organization for Standardization, Geneva, 2024, 46.
[26] S. E. Reed, J. L. Boggs, J. P. Mann, A GIS tool for modeling anthropogenic noise propagation in natural ecosystems, *Environmental Modelling & Software*, 2012, **37**, 1-5, doi: 10.1016/j.envsoft.2012.04.012.
[27] Y. Utepov, A. Imanov, Conceptual model of noise monitoring system for construction projects in cramped conditions, based on sensors and GIS, *Technobius*, 2022, **2**, 25, doi: 10.54355/tbus/2.3.2022.0025.
[28] V. Konbattulwar, N. R. Velaga, S. Jain, R. B. Sharmila, Development of in-vehicle noise prediction models for Mumbai Metropolitan Region, India, *Journal of Traffic and Transportation Engineering*, 2016, **3**, 380-387, doi: 10.1016/j.jtte.2016.04.002.
[29] E. Bocher, G. Guillaume, J. Picaut, G. Petit, N. Fortin, NoiseModelling: an open source GIS based tool to produce environmental noise maps, *ISPRS International Journal of Geo-Information*, 2019, **8**, 130, doi: 10.3390/ijgi8030130.
[30] G. Graziuso, A. B. Francavilla, S. Mancini, C. Guarnaccia, Open-source software tools for strategic noise mapping: a case study, *Journal of Physics: Conference Series*, 2022, **2162**, 012014, doi: 10.1088/1742-6596/2162/1/012014.
[31] C. Mydlarz, J. Salamon, J. P. Bello, The implementation of low-cost urban acoustic monitoring devices, *Applied Acoustics*, 2017, **117**, 207-218, doi: 10.1016/j.apacoust.2016.06.010.
[32] G. Lee, S. Moon, S. Chi, Real-time construction site noise mapping system based on spatial interpolation, *Journal of Management in Engineering*, 2023, **39**, 04022079, doi: 10.1061/jmenea.meeng-5089.
[33] M. Mir, F. Nasirzadeh, S. Lee, D. Cabrera, A. Mills, Construction noise management: A systematic review and directions for future research, *Applied Acoustics*, 2022, **197**, 108936, doi: 10.1016/j.apacoust.2022.108936.
[34] Google Maps, Satellite map of central Astana showing the construction site of the residential complex.
[35] Kazhydromet, The city of Astana and the Akmola region, Monthly newsletters on the state of the environment, Kazhydromet, Astana, June 29, 2024.
[36] S. J. Kim, H. Chang, J. Park, J. Kim, Design of a portable pneumatic power source with high output pressure for wearable robotic applications, *IEEE Robotics and Automation Letters*, 2018, **3**, 4351-4358, doi: 10.1109/LRA.2018.2864823
[37] Å. Björck, Least Squares methods, *Handbook of Numerical Analysis*, Amsterdam: Elsevier, 1990, **1**, 465-652, doi: 10.1016/s1570-8659(05)80036-5.
[38] C. C. Robusto, The cosine-haversine formula, *The American Mathematical Monthly*, 1957, **64**, 38, doi: 10.2307/2309088.
[39] M. Nurtas, Z. Zhantaev, A. Altaibek, S. Nurakynov, N. Mekebayev, K. Shiyapov, B. Iskakov, A. Ydyrys, Predicting the likelihood of an earthquake by leveraging volumetric statistical data through machine learning techniques, *Engineered Science*, 2023, **26**, 1031, doi: 10.30919/es1031.
[40] M. Nurtas, F. Tokmukhamedova, A. Ydyrys, Z. Zhantaev, S. Nurakynov, B. Iskakov, A. Altaibek, B. Matkerim, Application of finite element method for solving seismoacoustic modeling problems in poroelastic composite media, *Engineered Science*, 2023, **26**, 1030, doi: 10.30919/es1030.